THE JOURNAL OF BIOLOGICAL CHEMISTRY VOL. 290, NO. 13, pp. 8095–8109, March 27, 2015


# Upstream Binding of Idling RNA Polymerase Modulates Transcription Initiation from a Nearby Promoter*

Received for publication, November 24, 2014, and in revised form, February 2, 2015 Published, JBC Papers in Press, February 2, 2015, DOI 10.1074/jbc.M114.628131

**Veneta Gerganova[‡], Sebastian Maurer[‡1], Liubov Stoliar[‡], Aleksandre Japaridze[§], Giovanni Dietler[§], William Nasser[¶], Tamara Kutateladze[‖], Andrew Travers[**], and Georgi Muskhelishvili[‡2]**

*From the [‡]School of Engineering and Science, Jacobs University Bremen, Campus Ring 1, D-28759 Bremen, Germany, the [§]Laboratory of the Physics of Living Matter, EPFL, CH-1015 Lausanne, Switzerland, the [¶]UMR5240 CNRS/INSA/UCB, Université de Lyon, F-69003, INSA-Lyon, Villeurbanne, F-69621, France, the [‖]Ivane Beritashvili Centre of Experimental Biomedicine, Gotua str.14, Tbilisi, Georgia, and the **MRC Laboratory of Molecular Biology, Hills Road, Cambridge CB2 QH, United Kingdom*

**Background:** The *fis* promoter upstream region harbors RNA polymerase binding sites of unknown function.
**Results:** Modifications of the upstream polymerase binding affect *fis* gene expression in a supercoiling-dependent manner.
**Conclusion:** Concomitant binding of RNA polymerase at the *fis* promoter and upstream region acts as a topological device regulating transcription.
**Significance:** RNA polymerase can act as an architectural factor modulating the activity of transcription initiation complexes.

**The bacterial gene regulatory regions often demonstrate distinctly organized arrays of RNA polymerase binding sites of ill-defined function. Previously we observed a module of closely spaced polymerase binding sites upstream of the canonical promoter of the *Escherichia coli fis* operon. FIS is an abundant nucleoid-associated protein involved in adjusting the chromosomal DNA topology to changing cellular physiology. Here we show that simultaneous binding of the polymerase at the canonical *fis* promoter and an upstream transcriptionally inactive site stabilizes a RNAP oligomeric complex *in vitro*. We further show that modulation of the upstream binding of RNA polymerase affects the *fis* promoter activity both *in vivo* and *in vitro*. The effect of the upstream RNA polymerase binding on the *fis* promoter activity depends on the spatial arrangement of polymerase binding sites and DNA supercoiling. Our data suggest that a specific DNA geometry of the nucleoprotein complex stabilized on concomitant binding of RNA polymerase molecules at the *fis* promoter and the upstream region acts as a topological device regulating the *fis* transcription. We propose that transcriptionally inactive RNA polymerase molecules can act as accessory factors regulating the transcription initiation from a nearby promoter.**

Regulation of gene transcription by changes of the *Escherichia coli* RNA polymerase (RNAP)[3] holoenzyme composition and its association with transcription factors during the bacterial growth cycle is well understood (1, 2), whereas the role of the arrays of RNAP binding sites in the promoter regions is less appreciated. However, there is ample evidence that the flexibility of genetic regulation can be increased by organizing promoter arrays that are arranged in tandem and/or divergent orientation and often recognized by distinct holoenzymes (3–9). Conceivably, the promoter arrays not only enable the utilization of different RNAP holoenzymes for transcription but also facilitate the integration of multiple physiological signals under the changing growth conditions.

A number of studies in prokaryotes implicated the closely spaced arrays of RNAP binding sites in the regulation of both the strength and the pattern of gene transcription (10–14). Available data suggest that particular arrangements of the RNAP binding sites may have a regulatory function. For example, in the phage λ control region the RNAP molecules binding the closely spaced divergent promoters interfere with each other (15). Such interference was shown to provide an opportunity to regulate divergent genes by means of a single transcription factor binding between the promoters (16). Interference is not unique to divergent promoters, as the promoters arranged in tandem can also show strong transcriptional interference due to the pausing of the upstream initiating polymerase over the downstream promoter (17). Furthermore, in many cases the divergently oriented promoters can cooperate. For example, the diffusion of DNA negative supercoils induced in the wake of the translocating RNAPs (18) can mediate transcriptional coupling of the divergently transcribed operons leading to their coherent expression (19). Overall, during the last decade the role of closely spaced or overlapping promoters in genetic control became increasingly evident both in prokaryotes and eukaryotes (20–24), especially due to their preferential association with regulatory genes (25).

In addition to this regulatory complexity revealed in studies of individual promoter regions, recent genome-wide studies using chromatin immunoprecipitation (ChIP) approaches revealed a significant number of DNA-bound RNAP molecules that could not be associated with ongoing transcription (26–28), as well as numerous unusual promoter-like sites, or promoter "islands,"

* This work was supported by a grant from the Deutsche Forschungsgemeinschaft (to G. M.).
[1] Present address: Cell and Developmental Biology Program, Centre for Genomic Regulation (CRG), Universitat Pompeu Fabra, 08003 Barcelona, Spain.
[2] To whom correspondence should be addressed: Jacobs University Bremen, Campus Ring 1, D-28759 Bremen, Germany. Tel.: 49-421-200-3143; Fax: 49-421-200-3249; E-mail: g.muskhelishvili@jacobs-university.de.
[3] The abbreviations used are: RNAP, RNA polymerase; div, divergent; AFM, atomic force microscopy; qRT, quantitative RT; CAA, chloracetaldehyde; APTES, (3-aminopropyl)-triethoxysilane; CRP, cyclic AMP receptor protein.

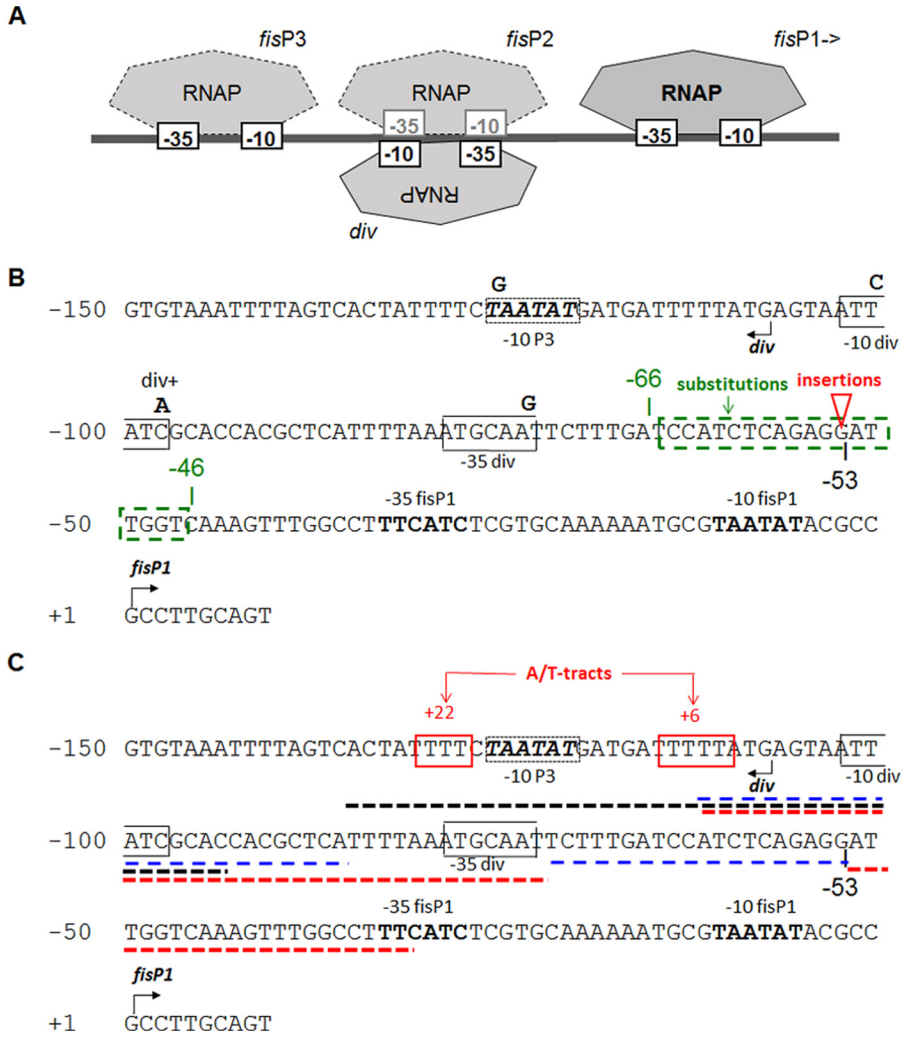


FIGURE 1. *A*, spatial arrangement of RNAP binding sites in the regulatory region of the *fis* operon. The orientation of binding sites is indicated by the order of the RNAP binding −10 and −35 elements. Note that the binding elements of the *fis*P2 site and *div* partially overlap. *Div* is a stronger binding site and stronger promoter when isolated on an episome compared with *fis*P2 (13), therefore we consider in the text only binding of *div*. Only *fis*P1 is considered to be engaged in active transcription *in vivo*. *B*, summary of the modifications in the *fis* promoter region. Substitutions in the −10 and −35 elements of *div* and −10 element of *fisP3* site (*italics*, *dashed box*) are indicated in *bold*; substitutions in the spacer between *fisP1* and *div* are *boxed* (*green dashed box*). The position of the 5G/C, 5A/T, and 10A/T insertions are indicted by the *red triangle*. *C*, sequence of the *fis* promoter region. The *div* −10 and −35 elements are *boxed*, and *fisP1* −10 and −35 elements are in *bold*. The IHF binding site is *underlined* (*black dashed line*). The CRP binding sites are *underlined* (*blue dashed lines*). The FIS binding regions are *underlined* (*red dashed lines*). The A/T tracts downstream of *div* are *boxed* (*red boxes*).

of unspecified biological function (29). The emergent view is that the genomic transcriptional landscape is much more complex than previously anticipated (30). Strikingly, over 90% of the identified *E. coli* gene promoters were found surrounded by other promoter-like signals (31). It is possible that these signals serve the purpose of enhancing the local concentration of RNAP in the vicinity of the promoter. However, it is also conceivable that closely spaced RNAP binding sites provide a device for engaging RNAP molecules into higher-order nucleoprotein complexes, analogous to recombination complexes involving multiple recombinase molecules binding adjacent DNA sites and acting both as regulatory and catalytic components of the complex (32–34).

The promoter of the *fis* operon encoding the abundant nucleoid-associated protein FIS belongs to so-called "stringently" controlled promoters (35) characterized by a GC-rich discriminator sequence between the −10 hexamer and the start point of transcription that endows it with exquisite sensitivity to DNA supercoiling (36). This is not surprising given that FIS is a global regulator involved in the homeostatic control of DNA supercoiling (37). The expression pattern of *fis* is remarkable and closely reflected in the variation of FIS protein abundance, which is accumulated in very large amounts (>50,000 copies) on the commitment of cells to growth in rich medium and thereafter sharply drops to about 1% of its maximal concentration (38). Previously, we identified an array of closely spaced polymerase binding sites organized in tandem and divergent (*div*) orientation upstream of the canonical *fis* promoter, denoted hereafter as *fis*P1 (Fig. 1*A*). Although potentially all these upstream sites could drive transcription when cloned in episomal reporter constructs, the observed array of RNAP binding sites was proposed to represent a regulatory module (13), consistent with the report that in the native chromosomal context they do not function as *bona fide* promoters (39). In keeping with this notion, mutation of the *div* site strongly binding the RNAP was found to affect the *fis*P1-driven production

of β-galactosidase *in vivo* (40). However, later studies revealed that the ORF of the first gene of the *fis* operon, *dusB*, is essential for the efficient translation of both the *fis* mRNA and the substituted reporter gene message (41–42), casting doubt on the results obtained with reporter constructs lacking the *dusB* ORF. Thus, the regulatory influence of the upstream binding of RNAP on *fis* expression remains unclear.

In this study we investigate the influence of the upstream binding of RNAP on *fis* expression. We show that RNAP forms a higher-order complex on simultaneous binding of the upstream and *fis*P1 sites *in vitro*, whereas modifications of the upstream sequence affect *fis*P1 transcription both *in vivo* and *in vitro*. This effect depends both on DNA supercoiling and the spatial arrangement of the upstream and *fis*P1 binding sites. Our observations strongly suggest that the upstream binding of idling RNAP plays a regulatory role in *fis* transcription.

## EXPERIMENTAL PROCEDURES

*Strains and Plasmids*—The *E. coli* K12 strain CSH50 ($F^-$ $\lambda^-$ *ara* Δ(*lac-pro*) *rpsL thi fimE*::*IS1*) was used throughout these experiments.

*Construction of pUCTER*—The *rrnB* terminator was PCR amplified from pBAD24 (primers 5′-CCCAAGCTTATAAAACGAAAGGCTCAGTCG-3′ and 5′-CGCGGATCCTCGAGCGGCCGCTAGCCCGGGATGCATCGCGAAAAAGGCCATCCGTCAGGATG-3′). The PCR product was digested by HindIII and BamHI and cloned into a HindIII/BamHI-digested pUC18 backbone. The *E. coli* CSH50 strain carrying a chromosomal *fisP-yfp* fusion was kindly provided by Dr. Berger and Alissa Respet. The *fisP-dusB-yfp-cat* and *fisP-yfp-cat* fragments were amplified with Phusion DNA Polymerase (Finnzymes) (primers 5′-GGTGGTCGCTAACATCCTTG-3′ and 5′-AGGAAACAGCTATGACCATG-3′), and subsequently KpnI digested and cloned into a SmaI/KpnI-digested pUCTER backbone. The resulting plasmid was subsequently sequenced and named pVG-fis4 (carrying *fisP-dusB-yfp-cat*) and pVG-fis6 (carrying *fisP-yfp-cat*). All point mutations and loop modifications were introduced with the Phusion Site-directed Mutagenesis kit (ThermoScientific) according to the manufacturer's recommendations. The loop modification constructs were amplified using primers homologous to the sequences flanking the *fis* operon locus and inserted in the native locus using the Red/ET recombination system. All plasmids and chromosomal insertions derived in this fashion were sequenced by Eurofins MWG Operon.

*Atomic Force Microscopy (AFM) Sample Preparation*—RNAP-DNA complexes were formed by incubating PCR-generated DNA fragments (primers 5′-AACAAATAGGGGTTCCGCGCA-3′ and 3′-GCTTTCATAACAACATTAAATGTGAGCGA-5′) and RNAP (Epicenter) at an equimolar ratio in 20 μl of AFM buffer (20 mM HEPES, pH 8.0, 50 mM KCl, 0.005% Tween, 4 mM $NiCl_2$) at 37 °C for 90 s. Following, the sample was transferred to a freshly cleaved mica disc (Plano Gmbh, Wetzlar). After incubation for 2 min the mica was rinsed 2 times by 1 ml of distilled, 0.2 μM filtered $H_2O$ and dried for 20 s under a weak flux of nitrogen.

*AFM Imaging of RNAP Complexes on Linear Fragments*—Images were acquired with a Multimode atomic force microscope equipped with a Nanoscope IIIa controller (Veeco Instruments GmbH, Germany), operating in tapping mode in air using a J-scanner and RTESP silicon cantilevers. Images of 512 × 512 pixels with a scan size of 2 × 2 μm were acquired at scan frequencies between 2 and 3 Hz. AFM images were processed by the NanoScope Image software (version 5.12r5; Veeco Instruments Inc., Santa Barbara, CA). Contour lengths of DNA molecules were determined manually with ImageJ software (version 1.32j by Wayne Rasband, NIH).

*APTES Modified Mica Surface*—For the APTES deposition the mica surface was functionalized with APTES in a separate step prior to DNA deposition. Pure APTES (≥98% purity) was purchased from Sigma and diluted in ultrapure water to a final concentration of 0.1 volume %. A 15-μl droplet of diluted APTES solution was deposited on freshly cleaved mica for 1 min, and then rinsed with 1 ml of ultrapure water, and finally dried using a gentle flow of compressed nitrogen.

*AFM of Plasmid DNA-RNAP Complexes on APTES*—RNAP-DNA complexes were formed by incubating TopoII-relaxed plasmid DNA molecules (final concentration ~0.5 ng/μl) and RNAP (final volume dilution of 1:2000) in 20 μl of P-buffer (1 mM Tris-HCl, pH 8.0, 10 mM KCl, 0.003% Tween, 2.5% glycerol, 4 mM $MgCl_2$) at 37 °C for 2 min. After depositing the RNAP/DNA mixture on the mica surface for 5 min the mica was rinsed with 1 ml of ultrapure water and finally dried using a gentle flow of compressed nitrogen.

*DNA Relaxation by Topoisomerase II*—2 μl of plasmid DNA (~100 ng/μl initial concentration) was incubated in a 20-μl volume using Topo Buffer and 1 μl of TOPO II (Affymetrix)I for 30 min at 37 °C, followed by heat inactivation of Topo II for 20 min at 65 °C.

*AFM Imaging of RNAP Complexes on Plasmids*—AFM images were collected using a MultiMode SPM with a Nanoscope III controller (Veeco Instruments, Santa Barbara, CA) operated in tapping mode in air. The AFM cantilevers used in air had a spring constant of 5 newton $m^{-1}$ (Bruker cantilevers, TAP150A) with resonance frequencies ranging between 120 and 160 kHz. All the recorded AFM images consist of 512 × 512 pixels with scan frequency ≤1 Hz. Images were simply flattened using Gwyddion* software (version 2.22) (83) and no further image processing was carried out.

*In Vitro Transcription*—The *in vitro* transcription reactions contained 500 ng of plasmid DNA as a template, 10 mM Tris-HCl, pH 8.0, 100 mM KCl, 10 mM $MgCl_2$, 1 mM DTT, 100 μg/ml of BSA, 8 nM RNA polymerase in a 50-μl volume. Reactions were preincubated for 10 min at 30 °C. Transcription reactions were initiated by adding 1/10 volume of 2.5 mM NTP mixture and incubated for 45 min at 30 °C. The reaction was stopped by adding 2 volumes of stop solution (1 mM EDTA, 50 mM sodium acetate, 0.2% SDS). Phenol extraction was followed by precipitation in the presence of 2 μg of glycogen, 0.3 M sodium acetate, and 2 volumes of ethanol. After precipitation and removal of residual ethanol, RNA was treated with TURBO DNase (Ambion) according to the manufacturer's recommendation.

*In Vitro $KMnO_4$ Reactivity Assay*—The reactions were assembled essentially as for the *in vitro* transcription assays. After 30 min of incubation at 30 °C, 0.02 volume of 100 mM potassium permanganate was added for 30 s. The reactions were stopped by addition of 0.02 volumes of β-mercaptoetha-

nol. After phenol extraction, the DNA was precipitated as described above and dissolved in water. This sample served as a template for 10 cycles of amplification by *Taq* polymerase with 5′-$^{32}$P radiolabeled primers 5′-GTAAATTTTAGTCACTATTTTC-3′ and 5′-ATTGTCCGATGCGCATGAGTTA-3′. The amplification products were analyzed on a 6% sequencing gel.

*In Vivo CAA Reactivity Assay*—Stationary CSH50 cells harboring the wild type and mutant *fis* promoter constructs (pWN1 and pWN1-div+ (13)) were diluted into fresh M9 minimal medium and grown for 30 min to an $A_{600}$ of 0.1 in 10 ml of medium supplemented with 4 g/liter of casamino acids. CAA was added for 10 min as described (46) to the batch cultures growing at 37 °C under vigorous shaking. The cells were collected by centrifugation and the plasmid DNA was extracted with QIAprep Spin Miniprep Kit. The isolated plasmids (500 ng) were used as a template for 5 cycles of PCR with *Taq* polymerase (New England Biolabs) and a $^{32}$P-labeled primer 5′-CTGAGCTGATATTGTCCG-3′ priming 60 bp downstream of the *fis* operon transcription initiation site. The samples were separated on a 6% denaturing polyacrylamide gel.

*RNA Extraction and Quantitative Real Time PCR*—RNA was extracted from batch cultures of cells grown in parallel to those used for the CAA reactivity assay. RNA was extracted with the RNAEasy® kit. The amount of transcript produced from *fis*P1 was measured by quantitative real time-PCR (qRT-PCR) with primers 5′-GCCTTGCAGTCACAGTATGG-3′ and 5′-ACGTCCGAAAAGGTCTGTCT-3′, amplifying the first 100 bp of the *fis*P1 transcript. The *yfp* transcript was measured from the strains carrying chromosomal insertions of the loop modifications with primers 5′-CGTGACCACCTTCGGCTAC-3′ and 5′-GAAGATGGTGCGCTCCTG-3′. qRT-PCR was carried out using QuantiTects SYBR Green one-step Q-PCR (Qiagen GmbH, Hilden, Germany), and a Mx3000PTM Real Time cycler (Stratagenes, La Jolla, CA). The PCR program consisted of the following cycles: 1 × 50 °C for 10 min; 1 × 95 °C for 15 min; and 40 × 95 °C for 30 s, 63 °C for 30 s, 72 °C for 30 s. The $\Delta\Delta C_t$ method was used for the quantification of the results (84),

$$R = \frac{\text{WT efficiency}^{C_t}}{\text{Target efficiency}^{C_t}} \quad \text{(Eq. 1)}$$

where WT is the reference sample. In the normalized expression level graphs, the ln of the derived *R* values were plotted. Thus a value of +1.0 and −1.0 indicate a 2-fold increase and decrease of expression, respectively.

*Treatment with Topoisomerase I*—The topoisomerase I treatment was performed under following conditions: 500 ng of DNA, 1× New England Biolabs 4 buffer, 1× BSA, and 0.5 μg of *Escherichia coli* topoisomerase I (kind gift of Monika Glynkowska). The reaction was performed at 37 °C for 30 min and stopped by heat inactivation (65 °C for 20 min).

*Nicking Reaction*—Nicking was performed with NtBspQI endonuclease (New England Biolabls). The reaction mixture contained 1 μg of DNA, 1 unit of enzyme, 1× New England Biolab 3 buffer. The mixture was incubated at 50 °C for 1 h and heat inactivated at 80 °C for 20 min.

*High-resolution Agarose Gel Electrophoresis*—The plasmid topoisomers were separated on 1% horizontal agarose gels run for 21 h at 45 V and 4 °C in 1× TBE buffer in the presence of 0.5 μg/ml of chloroquine. The DNA bands were visualized under UV light after staining with ethidium bromide.

*Real Time Promoter Activity Measurements*—All reporter plasmids were freshly transformed before each measurement. Bacterial strains carrying constructs inserted in the chromosomal loci were directly inoculated from glycerol stocks. The cells were grown on chloramphenicol LB agar plates for 18 h, after which several colonies were picked and grown in LB liquid medium overnight cultures for a maximum of 16 h. The measurements of the mutagenized pUC-fis4 were performed according to the following protocol. The cultures were diluted 1:1000 in a 96-well microtiter plate NUNC in LB medium and measured on time-resolved fluorometer Victor X5 technologies (PerkinElmer Life Sciences). Several colonies (4 to 5) were picked and analyzed per experiment. Fluorescence measurements were corrected with the background fluorescence of plasmid, carrying the fis6 construct (see Fig. 5). OD measurements were corrected with the respective medium blank. The cultures were diluted 1:200 in a 96-well microtiter plate NUNC in LB medium and measured on Tecan Infinite 200 Pro Plate Reader. Fluorescence measurements were corrected with the background fluorescence of the used parent CSH50 strain. OD measurements were corrected with the respective medium blank.

Absolute activity was defined as the product of the corrected fluorescence over the corrected $A_{580}$. The number of active hours is a value defined as the number of hours from time point 0 until the time point where the promoter activity loses oscillation. This represents the total number of hours when the main absolute activity peak is formed. The end point of the peak is the beginning of a plateau in the absolute activity representations. The measurements forming a plateau are selected as 12 or more consecutive time points whose respective values could be rounded to the same number, thus representing a "loss" in activity, because there are no fold-differences between the measurements. Data analysis was performed with Microsoft Excel. Graphs were generated via Origin Pro Lab 8.6. Error bars represent a S.E.

## RESULTS

*AFM Analyses of the RNAP-fis Promoter Interactions Reveal a Higher Order RNAP Complex*—We asked whether the specific arrangement of the RNAP binding sites in the *fis* promoter region supports formation of higher-order RNAP complexes. For this purpose we imaged the RNAP nucleoprotein complexes by AFM using a 816-bp DNA fragment comprising the *fis* promoter sequence from −108 to +106 with respect to *fis*P1 initiation start site at +1 flanked by vector sequences. On this fragment the upstream *div* site is located near the fragment center and *fis*P1 is closer to one end. Analysis of 434 RNAP-*fis*P1 complexes by AFM revealed a distinct variety of structures (Fig. 2, *A–E*). The measured diameter of a single RNAP molecule bound to DNA was 43 ± 5 nm, however, only 42% of all the complexes fitted these dimensions. Furthermore, ~13% of the complexes were about twice the diameter of a single RNAP molecule (Fig. 2*E*). To distinguish these complexes we generated three values designated A, B, and C for each measured

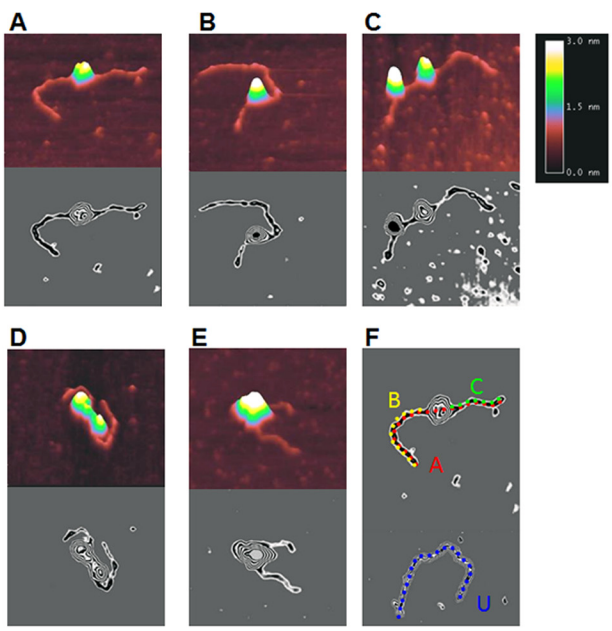


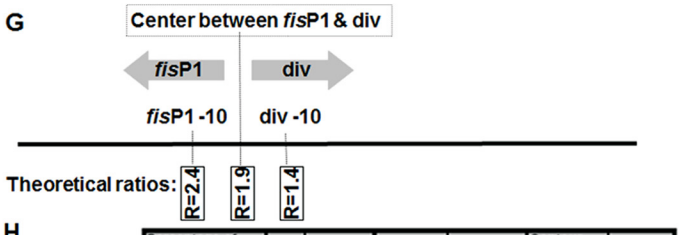


H

| | Percentage of total no. of complexes | Arm ratio | sd(±yEr) | Occupied space | sd(±yEr) | Contour length shortening | sd(±yEr) |
|---|---|---|---|---|---|---|---|
| *fis*P1 | 56% | 3.1 | 1.2 | 59.2 | 23.3 | 34.7 | 29.0 |
| *div* | 44% | 1.4 | 0.2 | 65.8 | 22.4 | 36.4 | 27.7 |
| >90nm occupied | 13% | 1.9 | 0.8 | 102.7 | 9.3 | 65.4 | 22.5 |

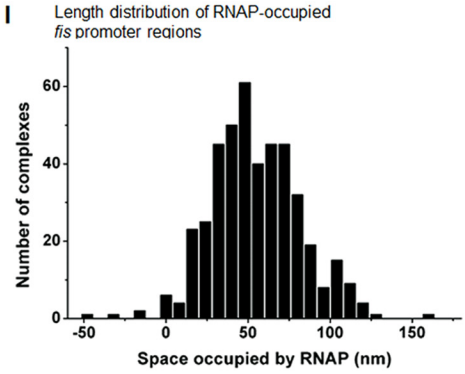


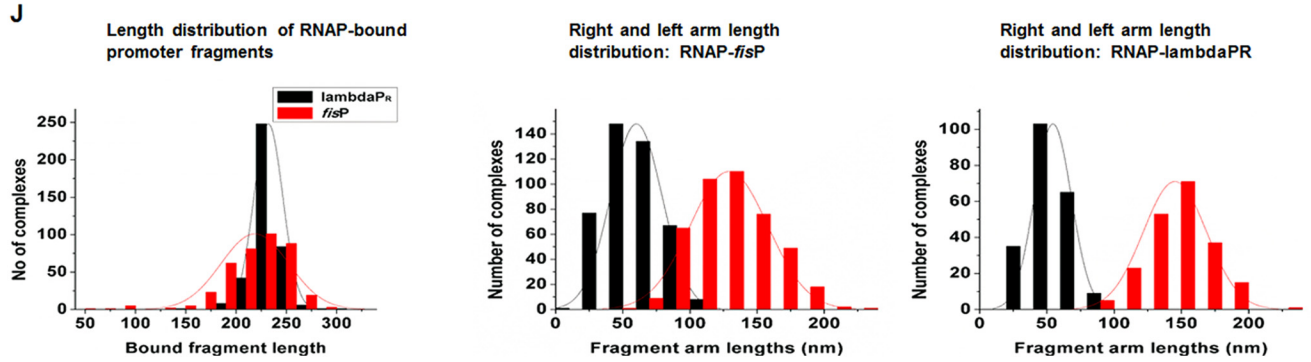


FIGURE 2. **AFM images of RNAP-*fis*P DNA complexes (260 × 260 nm, Z-scale 3 nm) and statistical data obtained for RNAP-*fis*P DNA complexes.** *A–E*, *upper panels* show the 70° angled views, *lower panels* show the top views. Note that two distinct positions (one more central, another near the DNA fragment end) are occupied by RNAP in *A* and *B*, whereas both positions appear occupied in the complex shown in *C–E*, the RNAP dimer complexes. *F*, statistical analysis of complexes. The parameters used for statistical analysis are indicated by *colored dotted lines*. *B* and *C*, arm lengths RNAP-*fis*P DNA complex, *A* = contour length of fragment with bound RNAP, and *U* = contour length of free DNA fragment. *G*, schematic of the *fis*P DNA fragment used for AFM. The assumed borderline between *fis*P1 and *div* binding sites (B/C arm ratio $r = 1.9$) and the location of corresponding −10 elements are indicated. *H*, summary of measurements of RNAP-*fis*P complexes. *I*, comparison of the distributions of DNA contour lengths in RNAP-*fis*P and the RNAP-λPR complexes (the λPR data taken for comparison (53)). *J*, distribution of the contour and arm lengths in the RNAP-fisP DNA and RNAP-λPR DNA complexes on linear fragments.

complex, where *A* and *U* represent the contour lengths of bound and unbound DNA, respectively (Fig. 2*F*). From these values the binding position (arm ratio B/C or C/B), the occupied space (U-B+C), and the DNA contour length shortening (U-A) were calculated.

Considering a distance of about 90 bp between the −10 hexamers of *fis*P1 and *div* we assume a separating borderline in the middle of this 90-bp sequence to distinguish *fis*P1 and *div* binding at a theoretical arm ratio of 1.9 (Fig. 2*G*). All complexes with higher arm ratios were assumed to be RNAP-*fis*P1 complexes (56% of total), whereas those with lower ratios (44% of total) were considered the RNAP-*div* complexes. We calculated the theoretical arm ratios for RNAP binding at *fis*P1 and *div* as 2.4 and 1.4, respectively. Our measurements indeed showed a ratio of 1.4 for RNAP-*div* complexes, but a higher ratio (3.1) was obtained for the RNAP-*fis*P1 complexes (Fig. 2*H*). This might be explained by differential wrapping of the DNA due to the bending anisotropy of the *fis* promoter region (43). Nevertheless, the average shortening of the contour length was around 35 nm in both cases, similar to that observed with the $\lambda P_R$ promoter (44). However, when we separately analyzed the complexes having twice (or more) the diameter of a single RNAP molecule we found an arm ratio of 1.9 and shortening of contour length by 65.4 nm (Fig. 2*H*). In general we observe a high variance of complexes formed on the *fis* promoter fragments (Fig. 2*I*) and a higher variance of contour length shortening and arm length distributions in comparison to the control $\lambda P_R$ promoter-RNAP complexes (Fig. 2*J*). The *div* site overlaps the *fis*P2 RNAP binding site (see Fig. 1*A*), and the higher variance could result from alternative binding of the *div* and *fis*P2 sites. How-

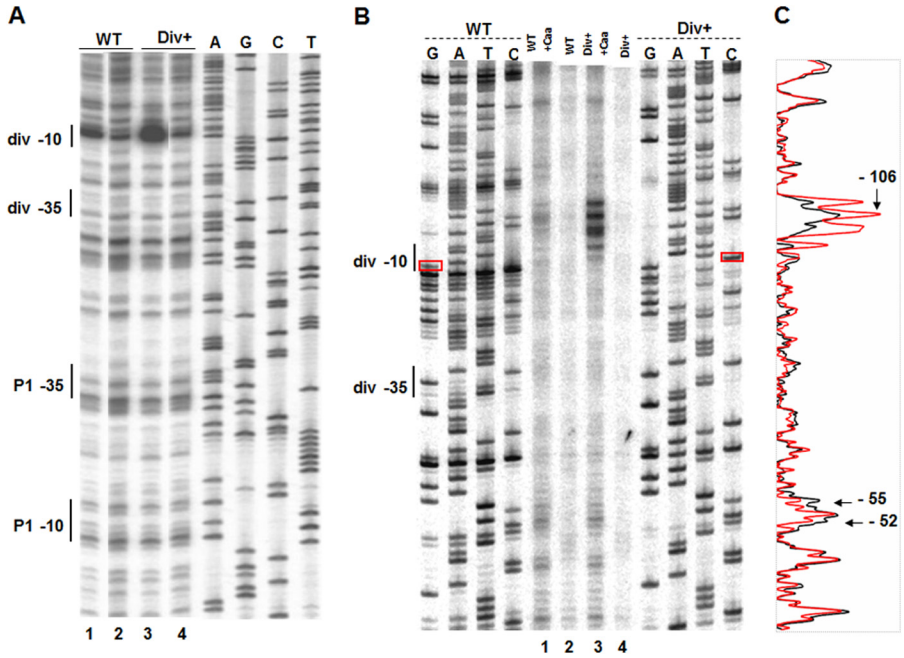


FIGURE 3. **RNAP binds the *div* site *in vitro* and *in vivo*.** *A*, *in vitro* $KMnO_4$ reactivity assay using the wild type and *div*+ promoter constructs. *Lanes 1* and *3*, $KMnO_4$ reactivity of the RNAP complexes formed at the wild type and *div*+ plasmid constructs, respectively. *Lanes 2* and *4* show the reactions with free DNA. *B, in vivo* CAA reactivity assay. The primer extension reactions using RNAs isolated from cells after CAA treatment are shown with corresponding sequencing reactions. *Lanes 1* and *3*, CAA reactivity of the wild type and *div*+ mutated *fis* promoter constructs, respectively. *Lanes 2* and *4* show the reactions with RNA isolated from untreated cells. The −10 and −35 elements of the *div* site are indicated. *Red boxes* indicate the positions of the *div*+ mutation and the original base. *C,* the overlay of scans of *lane 1* (*black*) and *lane 3* (*red*). Note the stronger untwisting in the −10 element of *div* carrying the *div*+ mutation.

ever, because RNAP tightly binds and readily untwists the *div* −10 region on linear fragments when no *fis*P2 untwisting is evident (40), we assume that RNAP predominantly binds at the *div* site. Taken together, these data are in keeping with previous findings showing that RNAP can simultaneously bind at the *fis*P1 and *div* sites *in vitro* (40) and demonstrate the formation of a higher-order complex on simultaneous binding of RNAP at *fis*P1 and the upstream transcriptionally inactive site.

*RNAP Binds the div Site in Vivo*—RNAP binds the div site with higher affinity than the *fis*P1 site *in vitro* (38), but whether this site is bound by RNAP *in vivo* is unclear. Previously we found that binding of RNAP strongly increases the potassium permanganate reactivity of the *div* −10 region *in vitro* indicative of DNA untwisting (40). To facilitate the detection of such an untwisting effect *in vivo* we introduced an "up" mutation in the *div* −10 element (hereafter designated div+) changing it to the consensus sequence (5′-GATAAT-3′ to 5′-TATAAT-3′). As expected, the div+ mutation increased the potassium permanganate reactivity of the DNA around the −10 element of *div* on binding of RNAP to plasmid constructs *in vitro* (Fig. 3*A*). No noticeable opening of the *fis*P1 was observed under the used conditions because "stringent" promoters need initiating nucleoside triphosphates for stable untwisting (45). To monitor the untwisting of the *div* site by RNAP *in vivo* instead of permanganate we used chloracetaldehyde (CAA) for modifying the bases in single-stranded DNA regions (46). After transformation of the wild type and div+ constructs in *E. coli*, the exponentially growing cells were treated with CAA for 10 min (see "Experimental Procedures"). The isolated plasmids were subjected to asymmetric PCR using a radiolabeled primer hybridizing 60 bp downstream of the *div* site. Visualization of the CAA reactivity signatures of the wild type and div+ promoter constructs on sequencing gels demonstrated that the div+ mutation strongly enhanced the reactivity of the *div* −10 element also *in vivo* (Fig. 3, *B* and *C*). We infer that the *div* site is capable of binding RNAP in the exponentially growing cells actively expressing *fis*.

*Mutations of Upstream RNAP Binding Sites Modulate the fisP1-driven Reporter Gene Expression in Vivo*—To test whether the upstream binding of RNAP has any physiological relevance, we investigated the effect of mutations in RNAP recognition elements of upstream sites on *fis* expression. Because recent studies showed that *dusB* is essential for the efficient translation of both the *fis* mRNA and the substituted reporter gene message (41, 42), we first generated the *fis* promoter constructs by substituting the *dusB* ORF (*fisP-yfp*) once and the *fis* ORF (*fisP-dusB-yfp*) once by the ORF of the yellow fluorescent protein (YFP) and examined the production of YFP from the promoter constructs inserted both in the chromosomal locus and also on the plasmids. We observed that lack of the *dusB* ORF on the *fisP-yfp* construct essentially abolished YFP production, whereas in the presence of *dusB* ORF the YFP expression showed a characteristic transient *fis* expression pattern (Fig. 4, *A* and *B*). We inferred that our *fisP-dusB-yfp* construct faithfully reproduces the *fis* expression pattern and can be safely used for further studies. In addition, we observed a direct correlation between the levels of YFP expression from plasmids and the duration of the lag period. A decrease in YFP expression leads to the shortening of the lag phase due to a lower YFP protein load, and vice versa, a higher YFP load results in a delay of growth (Figs. 4 and 5).

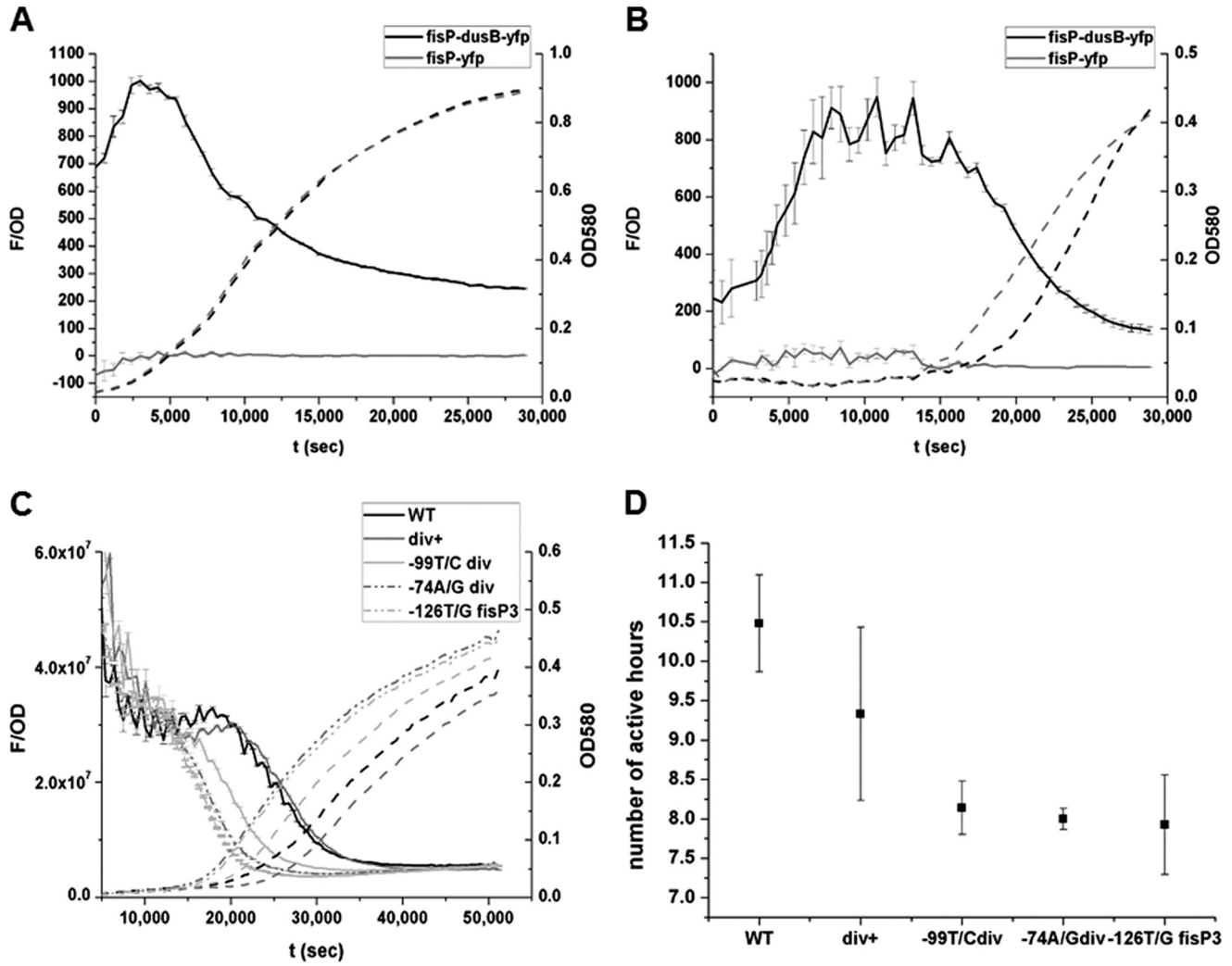


FIGURE 4. ***In vivo* analysis of the promoter activity of the native *fis*P1 region and mutations introduced upstream of the canonical *fis*P1.** *A,* absolute promoter activity (*fluorescence/OD580*) of constructs with and without the *dusB* ORF in the native chromosomal locus of *fis* over time. *B,* absolute promoter activity (*fluorescence/OD580*) of constructs with and without the *dusB* ORF, expressed from a plasmid backbone over time. *C* and *D,* div+ is an up mutation in the −10 region of *div*, −99T/C is a down mutation in the −10 region of *div*, −74A/G is a down mutation in the −35 region of *div*, and −126T/G is a down mutation introduced in the −10 region of *fis*P3. *C,* absolute promoter activity (*fluorescence/OD580*) of the mutated constructs over time. Note that all down mutations show a steep decline in promoter activity. Growth curves are depicted as *dashed line*, plotted on the right *y* axis. *D,* scatter plot of the number of active hours for each indicated sample. The value is calculated as the time (in hours) from the beginning of promoter activation until a detectable lack of oscillation (a plateau) of expression is reached. The faster loss of activity results in a smaller value of the number of active hours, as seen for all down point mutations.

To reveal the impact of the upstream RNAP binding on *fis* expression, we introduced mutations in the −10 and −35 elements of the *div* site (Fig. 1*B*) and tested them *in vivo*. The fluorescence produced from the wild type and mutant promoters was monitored during the entire growth cycle after the transformation of reporter constructs into *E. coli* K12 CSH50 cells. Clear effects were observed with "down" mutations in the −10 (5′-GATAAT-3′ to 5′-GATCAT-3′) and −35 (5′-TTGCAT-3′ to 5′-CTGCAT-3′) RNAP recognition elements of the *div* site, and also in the −10 element of the putative *fisP3* binding site (5′-TAATAT-3′ to 5′-GAATAT-3′) located upstream of *div*. This latter mutation was shown to increase the untwisting of the *div* −10 element by RNAP *in vitro* (13). The down mutations including those altering the *div* −10, *div* −35 recognition elements, and the *fisP3* −10 element significantly reduced YFP production, whereas *div*+ exerted no significant effect (Fig. 4, *C* and *D*). We infer that modulation of the upstream RNAP binding is relayed, either directly or indirectly, to the *fis*P1 promoter.

*Modifications of the Linker DNA between the Upstream Sites and fisP1 Modulate the fisP1-driven Reporter Gene Expression in Vivo and fisP1 Transcription in Vitro*—The *fis* promoter region contains binding sites for several regulatory proteins including FIS itself. The *fis*P3 −10 element overlaps with the IHF binding site, the *div* −10 element overlaps with the IHF binding site, CRP binding site II, and FIS binding site III, and the *div* −35 element overlaps with FIS binding site IV (40, 47). To minimize the possible interference with regulatory protein binding in the *fis*P1 upstream region we introduced insertions in the region between *fisP1* and the upstream RNAP sites, which did not alter the sequence of any of the FIS, CRP, or IHF binding sites (Fig. 1*C*). We introduced A/T-stretches corresponding to half a helical turn (5A/T) or a full turn (10A/T) of the DNA between positions −53 and −54 with respect to the start point of the *fis*P1 transcription initiation site at +1. The insertion point was located between the adjacent CRPI and FISII binding sites (40) in the center of the 40-bp sequence

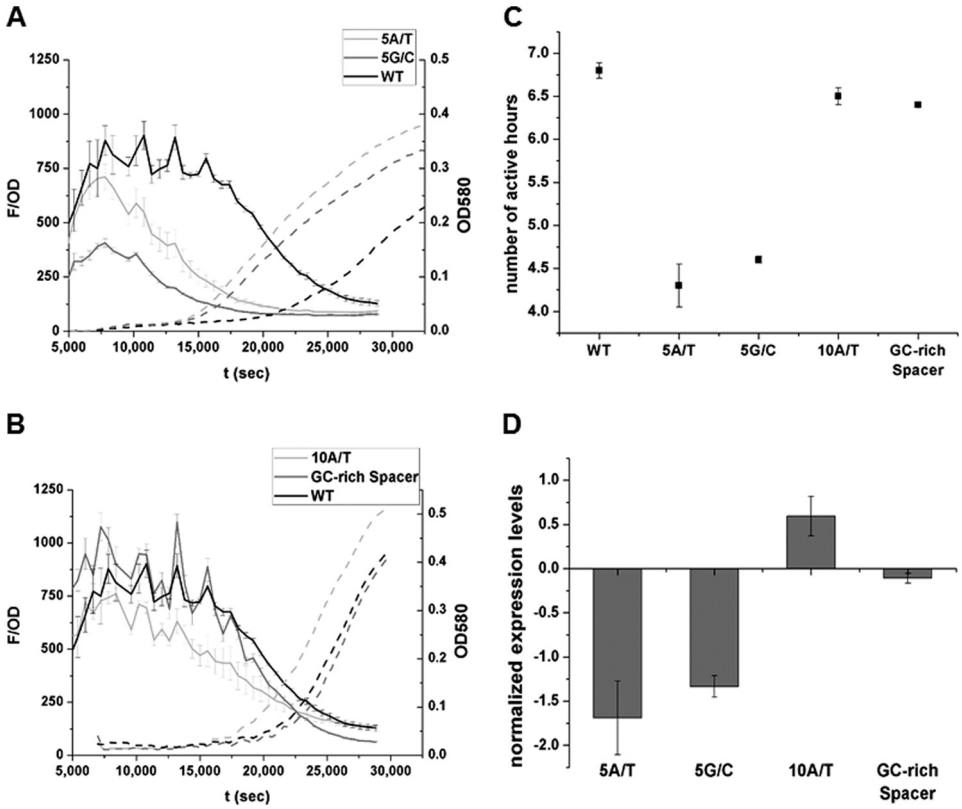


FIGURE 5. ***In vivo* and *in vitro* analysis of plasmid constructs carrying insertions and modifications in the *fis*P1 upstream region.** *A* and *B,* absolute promoter activity (*fluorescence/OD580*) of the constructs over time. Note that 5A/T and 5G/C show significantly lower expression levels in *A*, whereas 10A/T and GC-rich spacer constructs express *yfp* similarly to WT in plot (*B*). *C,* scatter plot of the number of active hours for each indicated sample. The value is calculated as the time (in hours) from the beginning of promoter activation until a detectable lack of oscillation (a plateau) of expression is reached. *D*, a qRT-PCR experiment with wild type serving as baseline. RNA was obtained from *in vitro* transcription. All raw data were analyzed with LinReg PCR software. Note that the negative values are due to plotting *ln* of the derived *R* values. A value of 1 indicates a twice higher product detection. All *error bars* are S.E. from at least four independent experiments.

separating the −35 RNAP hexamers of the *fis*P1 and *div* (Fig. 1, *B* and *C*). Because the inserted A/T stretches could be utilized by RNAP as fortuitous A + T-rich UP elements (48), we also inserted a stretch of five guanines (5G/Cs) in the same position. Notably, both the 5A/T and 5G/C insertions would alter the helical phasing between the bound polymerase molecules, whereas 10A/T would not. In addition, we substituted Gs for all Ts, and Cs for all As within a 19-bp region (positions −46 to −66 with respect to the start point of *fis*P1 transcription) between the *fis*P1 and *div* sites generating the "GC-rich spacer" construct, in which the thermodynamic stability of the DNA in the linker region between the divergent RNAP binding sites would be increased without altering their helical register (Fig. 1*C*).

All these constructs were tested for their influence on the *fis*P1 activity both *in vivo* and *in vitro*. Interestingly, we observed that both the 5A/T and 5G/C insertions significantly impaired *fis*P1 activity, insertion of a 10A/T had no noticeable effect, whereas the substitution of bases without altering the linker length (GC-rich spacer) only slightly decreased transcription (Fig. 5, *A–C*). Furthermore, when we tested these constructs *in vitro*, they showed a response fairly similar to the transcriptional response observed *in vivo* (Fig. 5*D*). Similar effects on *fis*P1 activity were observed when both the *yfp* mRNA and YFP protein expression strength of all these insertion constructs was tested in the native chromosomal context (Fig. 6, *A–C*). The finding that insertion of half, but not a full helical turn of the DNA exerted a negative effect on transcription suggested that spatial orientation of the upstream and the *fis*P1 RNAP binding sites is pertinent to the *fis*P1 transcriptional activity.

*Modifications of the Linker DNA between the div and fisP1 Sites Modulate the Supercoiling Response of fisP1 in Vitro*—Because *fis*P1 is exquisitely sensitive to DNA supercoiling (13, 36) we investigated the transcription efficiency of the wild type *fis* promoter and the 5A/T, 10A/T, and GC-rich spacer constructs using templates with different DNA superhelical density. We observed that the 5A/T insertion significantly lowered the activity of *fis*P1 at a high negative superhelical density, whereby this negative impact was abolished on the relaxed and nicked templates. In contrast, the 10A/T insertion was slightly more active, albeit to a different extent, on the supercoiled and relaxed templates, whereas the GC-rich spacer construct showed no significant differences to wild type (Fig. 7). The negative effect of the 5A/T insertion observed on supercoiled plasmids as opposed to the 10A/T and GC-rich spacer constructs, and its diminution with the loss of topological constraints, supports the notion that assembly of the productive transcription complex at *fis*P1 requires a specific local DNA geometry.

*Insertions in the div-fisP1 Linker DNA Region Affect the Promoter Untwisting by RNAP*—To reveal the functional relevance of the observed constraints imposed by local DNA geometry on

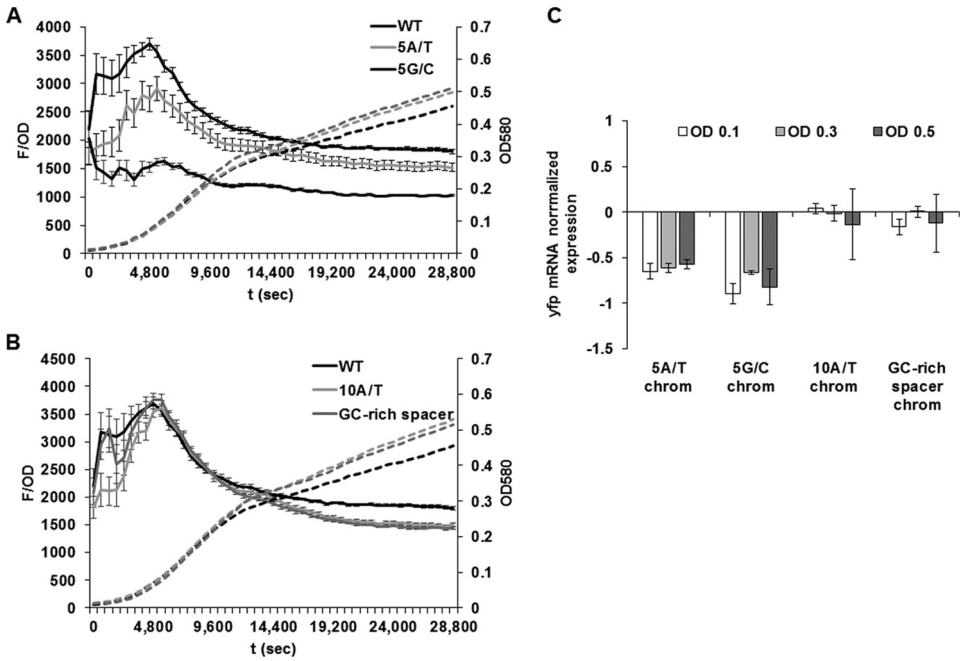


FIGURE 6. **Analysis of *fis*P1 promoter activity with chromosomal insertions of the 5A/T, 5G/C, 10A/T, and GC-rich spacer constructs.** A and *B*, absolute promoter activity (*fluorescence*/*OD580*) of the constructs over time. Note that 5A/T and 5G/C show significantly lower expression levels in *A*, whereas 10A/T and GC-rich spacer constructs express *yfp* similarly to WT in plot (*B*). Gain sensitivity was set to 100. *C*, a qRT-PCR experiment for *yfp* mRNA with wild type serving as baseline. The total RNA was extracted at intervals throughout the growth cycle (at $A_{600}$ 0.1, 0.3, and 0.5). All raw data were analyzed with LinReg PCR software. Note that the negative values are due to plotting the natural logarithm (*ln*) of the derived *R* values. A value of −1 indicates a twice lower product detection. All *error bars* are S.E.

the RNAP binding and transcriptional activity, we next investigated the effects of the insertions on promoter opening. The plasmid constructs were incubated with increasing RNAP concentrations and the promoter opening was monitored by potassium permanganate reactivity assay. Previously it was shown that the *div* site is readily untwisted at low RNAP concentrations, whereas higher RNAP concentrations are required for the untwisting of the stringent *fis*P1 promoter (13, 40). As expected, with all the used promoter constructs we observed a RNAP concentration-dependent untwisting of the −10 element of *div*, being most pronounced for the 10A/T insertion mutant (Fig. 8, *A* and *C*). The 10A/T construct also demonstrated a significantly increased untwisting of the *fis*P1 −10 element without much dependence on the RNAP concentration in the used range (25–75 nM). Higher RNAP concentrations were necessary to observe the opening of the wild type *fis*P1, whereas even at these high concentrations the promoter opening in both the 5A/T and 5G/C insertion constructs was strongly impaired (Fig. 8, *B* and *C*). Thus, whereas none of the 5-bp insertions impaired the *div* −10 hexamer untwisting, they both impaired the opening of the *fis*P1 promoter. We infer that the spatial organization of the *div* and *fis*P1 sites and thus, the local geometry of the DNA constrained by the RNAP nucleoprotein complex, is critical for the *fis*P1 promoter opening.

*Modifications of the Linker DNA between the div and fisP1 Sites Modulate the Binding of Plasmid Constructs by RNAP*—To understand the impact of the insertions on the RNAP nucleoprotein complex formation at the *fis* promoter we carried out AFM imaging experiments quantifying the RNAP binding to the plasmid constructs carrying the 5G/C, 5A/T, and 10A/T insertions, as well as the GC-rich spacer construct. To facilitate the visualization of the complexes, the plasmids were relaxed by Topo II before the complex formation and imaged on the APTES surface (see "Experimental Procedures"), which due to strong hydrophobic interactions traps the complexes more rapidly and thus better conserves their solution configuration (49, 50). At the used RNAP concentrations about 60–75% of plasmids were bound by a single RNAP molecule, whereas of the remaining 25–40% one-half were bound by two RNAP molecules and another half by two RNAP molecules in close vicinity, consistent with the putative oligomer. For the distinct constructs these distributions were not significantly different, whereas under the same conditions no significant RNAP binding was observed with plasmids lacking the *fis* promoter sequences (Fig. 9 and data not shown). The measurements of the arm ratios of complexes formed on linear fragments imaged on APTES at the same RNAP concentrations (Fig. 10) supported the notion that in complexes formed on plasmid constructs the RNAP was bound either at *div*, or *fis*P1, or both *div* and *fis*P1 sites.

We found that both the 5A/T and 5G/C plasmid constructs were significantly impaired in RNAP binding, whereas the 10A/T and GC-rich spacer constructs showed no difference to the wild type (Fig. 11). This significant difference in binding of the constructs differing only by modifications in the *fis* regulatory region indicates that we indeed observe the variation in occupation of the *div* and *fis*P1 sites and not of any plasmid-borne promoters. We thus infer that alteration of the spatial organization of RNAP binding sites by insertion of half a helical turn of the DNA between *div* and *fis*P1 interferes with RNAP binding.

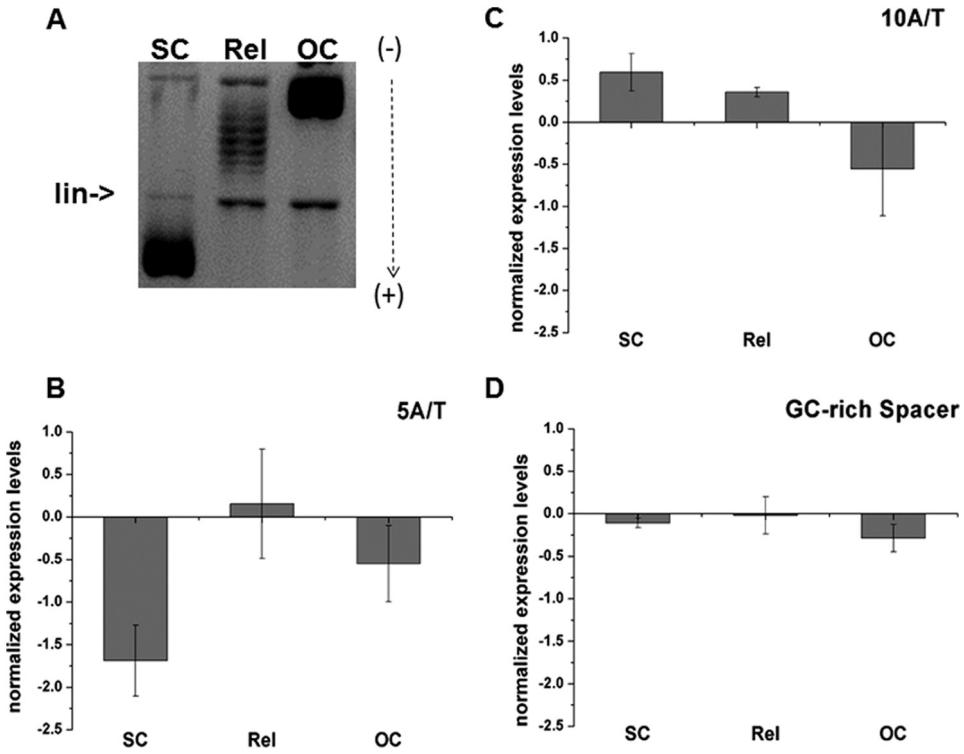


FIGURE 7. **Transcription from templates with different topology *in vitro*.** *A*, high resolution gel-electrophoresis of representative samples of the negatively supercoiled (*SC*), relaxed (*Rel*), and nicked (*OC*) templates used for transcription reactions shown in *B–D*. Migration of the linearized plasmid (*lin*) is indicated. *Dashed arrow* indicates the direction of the sample migration in the gel. The gel contained 0.5 $\mu$g/ml of chloroquine and therefore the migration of the negatively supercoiled species is retarded, whereas the relaxed population migrates as positively supercoiled species. The log ratios (*abscissa*) of the activities of 5A/T, 10A/T, and GC-rich spacer constructs are compared with the wild type (serving as baseline) under conditions of high negative superhelicity (*SC*), DNA relaxation (*Rel*), and on the nicked (*OC*) templates. The amount of the produced transcripts was measured by qRT-PCR. *B*, a qRT-PCR experiment measuring the transcription from the 5A/T insertion constructs using supercoiled (*SC*), relaxed (*Rel*), and nicked (*OC*) templates with wild type values serving as baseline. RNA was obtained from *in vitro* transcription. All raw data were analyzed with LinReg PCR software. Note that the negative values are due to plotting *ln* of the derived *R* values. A value of 1 indicates a twice higher product detection. All *error bars* are S.E. from at least three independent experiments. *C* and *D*, the same as *B* but for the 10A/T and GC-rich spacer constructs.

## DISCUSSION

In this study we describe the role of the upstream binding of RNAP in regulating the promoter of the *fis* operon encoding the pleiotropic regulator FIS (51, 52). By AFM imaging of complexes formed on linear promoter fragments we revealed a higher-order assembly consistent with a RNAP oligomer, presumably a dimer, as judged by the measurements of the contour length shortening, binding the divergently oriented *fis*P1 and *div* sites. The centers of the −10 RNAP binding elements of these divergent sites are separated by approximately nine helical turns, suggesting a particular local geometry of the complex with closely approaching RNAP molecules binding nearly on the same face of the DNA helix. We find that RNAP binding engages about 180 bp of DNA in this complex (Fig. 2), in good agreement with wrapping of about 90 bp observed for binding of individual RNAP molecules at the $\lambda P_R$ promoter (44, 53). Although it is difficult to translate these values into a three-dimensional structure, we surmise that in the complex the DNA spacer between the bound RNAP molecules is constrained.

Whether such a complex is readily formed *in vivo* is an open question. Although the propensity of the RNAP holoenzyme to dimerize is long known (54–57), the physiological relevance of this observation remains obscure. Interestingly, direct physical interactions by "head to tail" stacking of core RNAP molecules have been implicated in facilitating transcription elongation (58, 59), whereas a more recent observation suggested formation of transcriptionally active dimers by interactions between the RNAP core enzymes stacking "side by side" (60). It is noteworthy that the early electron microscopy observations of a V-shaped structure of the RNAP dimer,[4] as well as the structure of a dimer unit observed in recent crystallographic studies (61, 62) would be consistent with the possibility of physical interactions between the RNAP molecules binding the divergent *fis*P1 and *div* sites.

*Relevance of the Upstream RNAP Binding and the Spatial Arrangement of the Upstream and fisP1 Sites to fis Transcriptional Control*—Our data suggest that the upstream binding of RNAP has a role in the control of *fis* expression. First, we found that up-mutation in the *div* site (*div*+) increased the untwisting of the *div* −10 element *in vivo* (Fig. 3), indicating that this site can be occupied by polymerase during the exponential growth when the expression of *fis* is maximal (35, 38). Second, point mutations affecting the RNAP binding consensus sequences of the *div* and *fis*P3 sites modulated the *fis*P1 transcription, albeit to a different extent (Fig. 4, *C* and *D*). Importantly, the RNAP recognition elements of the *div* site partially overlap those of the *fis*P2 site, organized in tandem with *fis*P1 (see Fig. 1*A*). However, because *div* is both a stronger binding site readily

[4] J. T. Finch and A. Travers, unpublished observations.

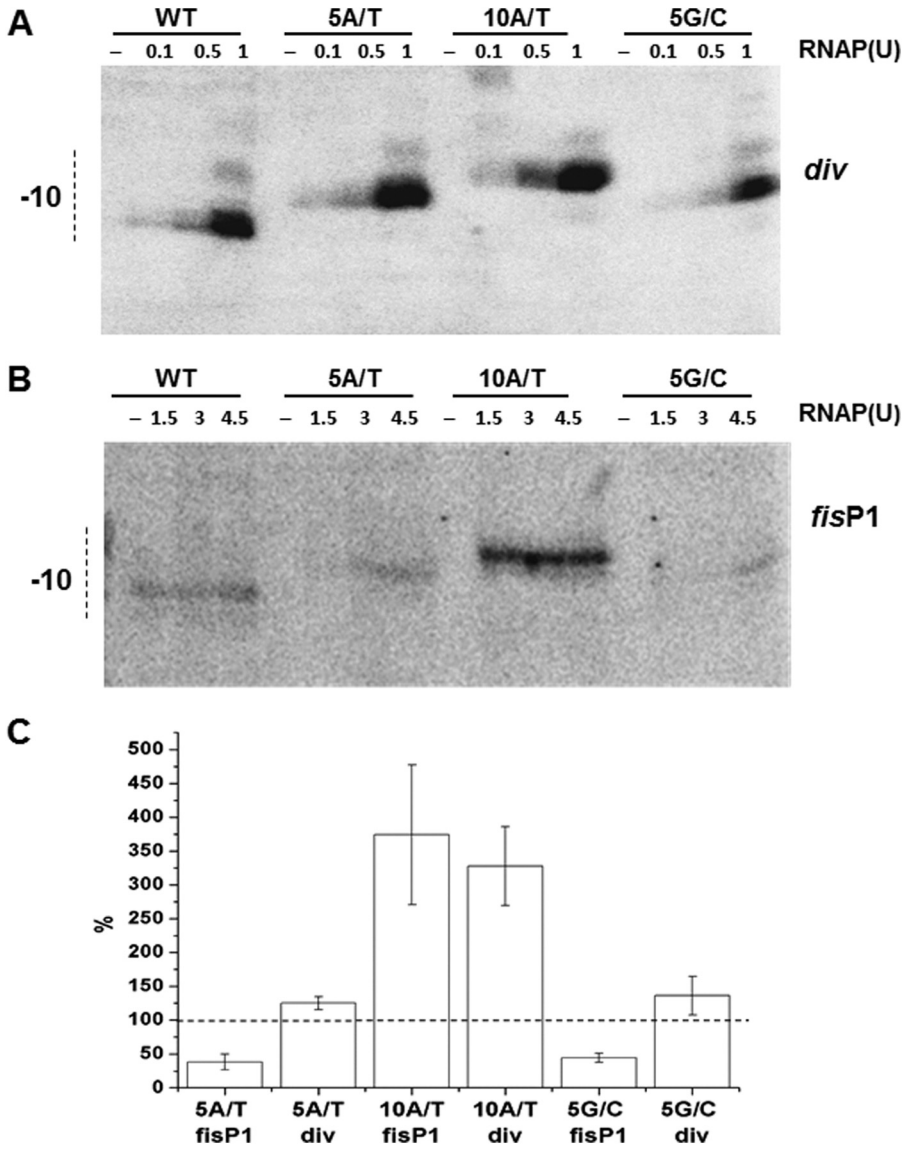


FIGURE 8. **Potassium permanganate reactivity of the *fis*P1 and *div* complexes formed on plasmid constructs *in vitro*.** *A* and *B*, Phosphorimager scan of a representative gel showing the permanganate reactivity of the −10 elements of the *div* site (*A*) and *fis*P1 (*B*) detected for the wild type (*WT*), 5A/T, 10A/T, and 5G/C insertion constructs at different RNAP concentrations indicated in units (1 unit = 16 nM RNAP). *C*, statistics derived from four independent experiments. The band intensity for each sample at each RNAP concentration was normalized to that of wild type (WT *div* or WT *fis*P1) set to 100%. In the presented quantification an average of the detected individual mutant to wild type signal ratios over all the RNAP concentrations is shown. All data analysis was done using the AIDA software and Microsoft Excel.

forming open complexes *in vitro* (Fig. 3) and acts as a substantially stronger promoter than *fis*P2 when isolated from native chromosomal context on plasmid constructs *in vivo* (13), we assume that these mutations primarily affect *div* binding. We cannot rule out that these mutations affect the binding of transcriptional regulators of *fis* expression the binding sites of which overlap the *div* and *fis*P3 RNAP binding elements including FIS itself, the global repressor H-NS (63), and the pleiotropic regulators IHF and CRP (Fig. 1*C*). This complex question merits separate study and is out of the scope of this paper. The effects of disruptions in the helical phasing of FIS binding sites on transcription have been previously studied (64). It was shown that the assembly of a specific nucleoprotein complex, comprising a regulatory protein, RNAP, and DNA, requires three helically phased FIS binding sites in the promoter upstream region. In the case of the *fis* promoter region, however, the multitude of regulators and the entanglement of their binding sequences with those of the RNAP required the use of insertion mutations, which did not affect any of the known regulator binding sites. We observed a coherent response of the *fis*P1 promoter to the insertion mutations both on plasmids and in the chromosomal context *in vivo* and also *in vitro* (Figs. 5 and 6) with only the insertions of half a helical turn (5A/T and 5G/C) but not the full turn (10A/T) of DNA decreasing the *fis*P1 activity.

In *E. coli* the A + T-rich UP elements binding the C-terminal domain of the RNAP $\alpha$ subunit are normally located between positions −40 and −60 from the transcription start point (48). At *fis*P1 a sequence between positions −52 and −39 ($^{-52}$ATTGGTCAAAGTTT$^{-39}$) could serve as a presumptive proximal UP element-like subsite, but this is unlikely because the substitutions of Gs for Ts and Cs for As in this sequence in

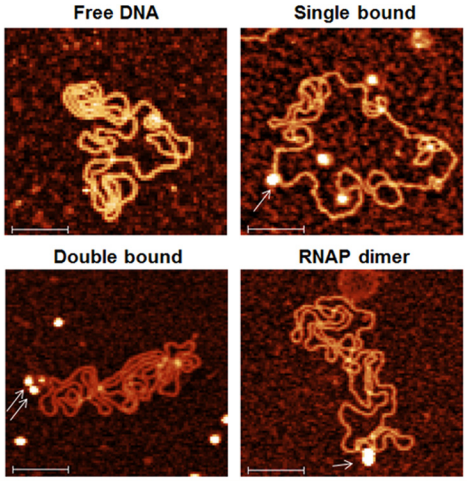


| Constructs | N | Double bound | Single bound | Dimers |
|---|---|---|---|---|
| WT | 55 | 20 ± 5% | 65 ± 5% | 15 ± 5% |
| 5A/T | 35 | 15 ± 5% | 75 ± 5% | 10 ± 5% |
| 5G/C | 35 | 15 ± 5% | 70 ± 5% | 15 ± 5% |
| 10A/T | 55 | 20 ± 5% | 60 ± 5% | 20 ± 5% |
| GC-rich Spacer | 55 | 20 ± 5% | 60 ± 5% | 20 ± 5% |

FIGURE 9. **Specific DNA complexes formed by RNAP with plasmids on the APTES surface.** Representative images show the free plasmid (wild type) DNA and the complexes formed on the same DNA after incubation with RNAP. In AFM images the DNA was considered bound by RNAP only when the height measured at any point of the DNA molecule was at least 3 nm higher than the average height measured for the free DNA (3 nm corresponds to the minimum height of the RNAP monomer). By this criterion in the representative image only the complexes indicated by the *white arrows* are assumed bound. The RNAP-DNA complexes were formed by incubating the plasmid DNA molecules relaxed by TopoII with RNAP. The measurements and the statistical analysis of complexes were as described under "Experimental Procedures."

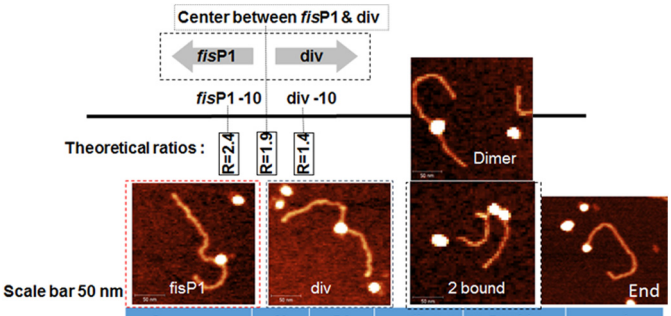


| Constructs | N | P1 | div | Double bound | end binding |
|---|---|---|---|---|---|
| WT | 115 | 31% | 11% | 9% | 49% |
| 5A/T | 105 | 33% | 15% | 6% | 46% |
| 5G/C | 110 | 32% | 19% | 12% | 37% |
| 10A/T | 110 | 17% | 12% | 16% | 55% |
| GC-rich Spacer | 90 | 25% | 19% | 9% | 47% |

FIGURE 10. **Specific DNA complexes formed by RNAP on linear *fis* DNA fragments on the APTES surface.** Representative images show the complexes formed on the linear DNA after incubation with RNAP. The parameters used for the statistical analyses of complexes were the same as described in the legend to Fig. 2. Under these conditions 37–55% of fragments demonstrated end binding.

the GC-rich spacer construct ($^{-52}$CGGGGGCAAAGTTT$^{-39}$) did not impair *fis*P1 activity in a purified *in vitro* system (Fig. 5*D*). In principle, the 5A/T and 10A/T insertions, which are located upstream of this sequence (at position −53; Fig. 1*B*),

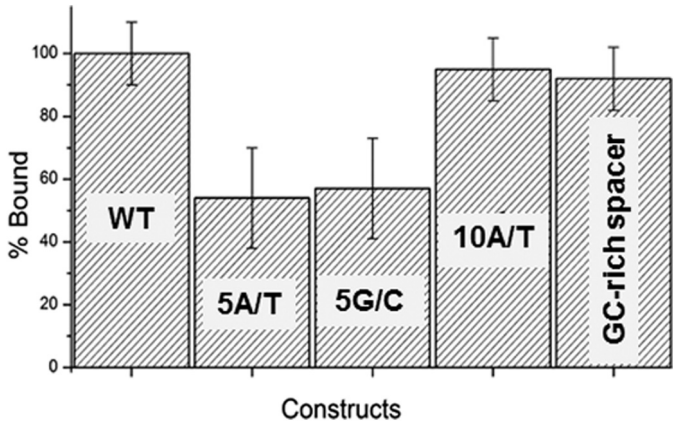


FIGURE 11. **Binding of RNAP at the plasmid constructs and representative AFM images of Plasmid DNA-RNAP complexes.** Quantification of RNAP binding to plasmid DNA. The columns are based on analyses of 100 DNA-RNAP complexes for each modified promoter construct. The standard *error bars* indicate the variation in the number of "bound" *versus* "unbound" DNA molecules based on the individual AFM images for a given DNA-RNAP complex.

could create a fortuitous UP element. However, such a fortuitous UP element would be expected to exert a strong activating effect on *fis*P1 as observed with other stringent promoters (65), whereas for the 10A/T insertion we observed either no effect, or only moderate activation, respectively, *in vivo* and *in vitro*, and for the 5A/T insertion construct we observed an inhibition. In addition, not only the 5A/T, but also the 5G/C insertion elicited inhibitory effects both *in vivo* and *in vitro*. Because the primary contribution to the C-terminal domain of the RNAP $\alpha$ subunit binding is mediated via the interactions with the DNA minor groove (66), and because the 5A/T and 5G/C sequences would have a substantially different (narrow and wide, respectively) minor groove geometry (67), our data suggest that it is not the specific sequence, but rather its extent, that is relevant.

We suggest that the insertion mutations modulate *fis*P1 transcription by altering the spatial organization of the RNAP upstream and *fis*P1 binding sites. This notion is supported by several lines of evidence. First, we observed that insertions of one-half but not a full helical turn of DNA impair *fis*P1 transcription. Second, the substitution of bases within a 19-bp sequence in the linker DNA between the divergent *fis*P1 and *div* sites without altering their helical arrangement (GC-rich spacer construct) does not affect *fis*P1 transcription *in vitro* and is less detrimental than the 5A/T and 5G/C insertions (Figs. 5 and 6). Furthermore, this dependence of promoter activity on helical phasing is lost if the plasmid DNA is relaxed by topoisomerase action or by DNA nicking. This latter observation is especially relevant, because *fis*P1 is a highly supercoiling-dependent promoter (13, 68), whereas supercoiling affects the preferred helical repeat and so the local geometry of the DNA (67). In addition, we observe that on plasmid constructs the 5A/T and 5G/C insertion mutants are significantly impaired in RNAP binding (Fig. 11). Finally, we observe that the 5-bp insertion mutants are also impaired in the open complex formation at *fis*P1, despite the untwisting of the *div* −10 element DNA being fairly similar to wild type (Fig. 8). Taken together these observations strongly suggest that the alteration of local geometry of the DNA in the *div-fis*P1 linker region destabilizes the binding of the RNAP at

*fis*P1 thus preventing productive transcription complex formation. The effect of the 10A/T insertion is in keeping with this notion. This insertion would increase the flexibility of the linker DNA between the divergent promoters by virtue of its extension without compromising the helical phasing and so partially relieve the constraints imposed by local DNA geometry. Indeed, we observed that the 10A/T insertion increased the untwisting of the *div* and *fis*P1 −10 elements without enhancing the RNAP binding on plasmid constructs (compare Figs. 8 and 11).

In contrast to the *fis*P1 promoter, the *div* site is not associated with a meaningful ORF and is poorly, if at all, transcribed *in vivo* (39). Our data confirms previous observations demonstrating that RNAP tightly binds and readily untwists the *div* −10 region under conditions when no *fis*P1 untwisting is evident (40). But why is the strong *div* RNAP binding site not active as a promoter *in vivo*? One plausible explanation is the existence of short A/T tracts centered at +6 and +22 downstream from the *div* start site (see Fig. 1*C*). Such sequences were postulated to trap polymerase acting as strong pausing sites (69). Indeed, deletion of the downstream A/T tracts renders *div* a strong promoter *in vivo*, whereas the *div* activity cannot be detected on constructs retaining the downstream region (13, 39). In this respect the *div* site is reminiscent of those promoters that are rate-limited at the clearance step (70).

*Implications*—Is there any physiological rationale for the upstream RNAP binding in the *fis* promoter region? FIS is a pleiotropic regulator coupling the global cellular physiology with chromosomal DNA dynamics and boosting the ribosome production and growth on the entry of cells into exponential phase (68, 71). Expression of *fis* depends on the richness of the medium (72) and oxygen availability (9), whereas inactivation of *fis* leads to reduction of growth rate (73). Importantly, whereas the transcription machinery and the DNA superhelicity are coupled and vary with cellular physiology (74–76), the *fis* promoter is thought to act as a sensor and transmitter of the global supercoiling state (77). This notion is supported by a recent finding of an upstream *fis* transcription initiation site in *Salmonella* suggesting that the *fis* regulatory region acts as a topological switch sensing the cellular physiology (9). Furthermore, the *fis*P upstream sequence is highly conserved in various pathogenic *E. coli* and *Shigella* strains (data not shown). We propose that the supercoiling-dependent stabilization of a particular local DNA geometry in the *fis* promoter region serves as a device for sensing free superhelical energy and transmitting the information to the RNAP nucleoprotein complex, whereas upstream binding of RNAP at suboptimal superhelical densities precludes productive transcription complex formation. This basic regulation mechanism could be fine-tuned not only by alterations of RNAP concentration and/or $\sigma$ factor composition, but also by binding of regulatory proteins and small regulatory molecules, including the initiation of nucleoside triphosphates (13, 35, 36, 74, 76, 78, 79).

Our study together with previous reports of multiple RNAP binding sites in the control regions of the pleiotropic regulators (11, 12) suggests that adjacent binding and interaction of the RNAP molecules may provide a versatile mechanism for direct sensing of physiological conditions by the pleiotropic genetic loci. This is in keeping with exquisite sensitivity of the divergent promoters to supercoiling and topoisomerase action (80, 81). We believe that exploration of the interactions of closely spaced RNAP binding sites in other model systems, including eukaryotes (25, 82), will provide important insights into the complexity of the transcriptional regulatory system and its evolution.

*Acknowledgment—We thank Prof. Jürgen Fritz for providing the AFM facility.*

## REFERENCES


1. Ishihama, A. (2000) Functional modulation of *Escherichia coli* RNA polymerase. *Annu. Rev. Microbiol.* **54,** 499–518
2. Ishihama, A. (2012) Prokaryotic genome regulation: a revolutionary paradigm. *Proc. Jpn. Acad. Ser. B Phys. Biol. Sci.* **88,** 485–508
3. Tse-Dihn, Y. C., and Beran, R. K. (1988) Multiple promoters for transcription of the *Escherichia coli* DNA topoisomerase I gene and their regulation by DNA supercoiling. *J. Mol. Biol.* **202,** 735–742
4. Lesley, S. A., Jovanovich, S. B., Tse-Dinh, Y. C., and Burgess, R. R. (1990) Identification of a heat shock promoter in the topA gene of *Escherichia coli*. *J. Bacteriol.* **172,** 6871–6874
5. Goodrich, J. A., and McClure, W. R. (1991) Competing promoters in prokaryotic transcription. *Trends Biochem. Sci.* **16,** 394–397
6. Liebig, B., and Wagner, R. (1995) Effects of different growth conditions on the *in vivo* activity of the tandem *Escherichia coli* ribosomal RNA promoters P1 and P2. *Mol. Gen. Genet.* **249,** 328–335
7. Qi, H., Menzel, R., and Tse-Dinh, Y. C. (1997) Regulation of *Escherichia coli topA* gene transcription: involvement of a $\sigma$S-dependent promoter. *J. Mol. Biol.* **267,** 481–489
8. Govantes, F., Orjalo, A. V., and Gunsalus, R. P. (2000) Interplay between three global regulatory proteins mediates oxygen regulation of the *Escherichia coli* cytochrome *d* oxidase (cydAB) operon. *Mol. Microbiol.* **38,** 1061–1073
9. Cameron, A. D., Kröger, C., Quinn, H. J., Scally, I. K., Daly, A. J., Kary, S. C., and Dorman, C. J. (2013) Transmission of an oxygen availability signal at the *Salmonella enterica* serovar *Typhimurium fis* promoter. *PLoS One* **8,** e84382
10. Le Grice, S. F., and Sonenshein, A. L. (1982) Interaction of *Bacillus subtilis* RNA polymerase with a chromosomal promoter. *J. Mol. Biol.* **162,** 551–564
11. Hanamura, A., and Aiba, H. (1991) Molecular mechanism of negative autoregulation of *Escherichia coli crp* gene. *Nucleic Acids Res.* **19,** 4413–4419
12. González-Gil, G., Kahmann, R., and Muskhelishvili, G. (1998) Regulation of crp transcription by oscillation between distinct nucleoprotein complexes. *EMBO J.* **17,** 2877–2885
13. Nasser, W., Rochman, M., and Muskhelishvili, G. (2002) Transcriptional regulation of *fis* operon involves a module of multiple coupled promoters. *EMBO J.* **21,** 715–724
14. Li, M., Wang, J., Geng, Y., Li, Y., Wang, Q., Liang, Q., and Qi, Q. (2012) A strategy of gene overexpression based on tandem repetitive promoters in *Escherichia coli*. *Microb. Cell Fact.* **11,** 19
15. Strainic, M. G. Jr., Sullivan, J. J., Collado-Vides, J., and deHaseth, P. L. (2000) Promoter interference in a bacteriophage lambda control region: effects of a range of interpromoter distances. *J. Bacteriol.* **182,** 216–220
16. El-Robh, M. S., and Busby, S. J. (2002) The *Escherichia coli* cAMP receptor protein bound at a single target can activate transcription initiation at divergent promoters: a systematic study that exploits new promoter probe plasmids. *Biochem. J.* **368,** 835–843
17. Palmer, A. C., Ahlgren-Berg, A., Egan, J. B., Dodd, I. B., and Shearwin, K. E. (2009) Potent transcriptional interference by pausing of RNA polymerases over a downstream promoter. *Mol. Cell* **34,** 545–555
18. Liu, L. F., and Wang, J. C. (1987) Supercoiling of the DNA template during transcription. *Proc. Natl. Acad. Sci. U.S.A.* **84,** 7024–7027

19. Opel, M. L., and Hatfield, G. W. (2001) DNA supercoiling-dependent transcriptional coupling between the divergently transcribed promoters of the ilvYC operon of *Escherichia coli* is proportional to promoter strengths and transcript lengths. *Mol. Microbiol.* **39,** 191–198
20. Yamada, M., Kabir, M. S., and Tsunedomi, R. (2003) Divergent promoter organization may be a preferred structure for gene control in *Escherichia coli*. *J. Mol. Microbiol. Biotechnol.* **6,** 206–210
21. Bae, J. Y., Laplaza, J., and Jeffries, T. W. (2008) Effects of gene orientation and use of multiple promoters on the expression of XYL1 and XYL2 in *Saccharomyces cerevisiae*. *Appl. Biochem. Biotechnol.* **145,** 69–78
22. Nakagawa, H., Tategu, M., Yamauchi, R., Sasaki, K., Sekimachi, S., and Yoshida, K. (2008) Transcriptional regulation of an evolutionary conserved intergenic region of CDT2-INTS7. *PLoS One* **3,** e1484
23. Seila, A. C., Core, L. J., Lis, J. T., and Sharp, P. A. (2009) Divergent transcription: a new feature of active promoters. *Cell Cycle* **8,** 2557–2564
24. Uesaka, M., Nishimura, O., Go, Y., Nakashima, K., Agata, K., and Imamura, T. (2014) Bidirectional promoters are the major source of gene activation-associated non-coding RNAs in mammals. *BMC Genomics* **15,** 35
25. Lepoivre, C., Belhocine, M., Bergon, A., Griffon, A., Yammine, M., Vanhille, L., Zacarias-Cabeza, J., Garibal, M. A., Koch, F., Maqbool, M. A., Fenouil, R., Loriod, B., Holota, H., Gut, M., Gut, I., Imbert, J., Andrau, J. C., Puthier, D., and Spicuglia, S. (2013) Divergent transcription is associated with promoters of transcriptional regulators. *BMC Genomics* **14,** 914
26. Grainger, D. C., Hurd, D., Harrison, M., Holdstock, J., and Busby, S. J. (2005) Studies of the distriution of *Escherichia coli* cAMP-receptor protein and RNA polymerase along the *E. coli* chromosome. *Proc. Natl. Acad. Sci. U.S.A.* **102,** 17693–17698
27. Reppas, N. B., Wade, J. T., Church, G. M., and Struhl, K. (2006) The transition between transcriptional initiation and elongation in *E. coli* is highly variable and often rate limiting. *Mol. Cell* **24,** 747–757
28. Mooney, R. A., Davis, S. E., Peters, J. M., Rowland, J. L., Ansari, A. Z., and Landick R. (2009) Regulator trafficking on bacterial transcription units *in vivo*. *Mol. Cell* **33,** 97–108
29. Shavkunov, K. S., Masulis, I. S., Tutukina, M. N., Deev, A. A., and Ozoline, O. N. (2009) Gains and unexpected lessons from genomes-scale promoter mapping. *Nucleic Acids Res.* **37,** 4919–4931
30. Wade, J. T., and Grainger, D. C. (2014) Pervasive transcription: illuminating the dark matter of bacterial transcriptomes. *Nat. Rev. Microbiol.* **12,** 647–653
31. Huerta, A. M., Francino, M. P., Morett, E., and Collado-Vides, J. (2006) Selection for unequal densities of $\sigma$70 promoter-like signals in different regions of large bacterial genomes. *PLoS Genetics* **2,** e185
32. Murley, L. L., and Grindley, N. D. (1998) Architecture of the $\gamma\delta$ resolvase synaptosome: oriented heterodimers identity interactions essential for synapsis and recombination. *Cell* **95,** 553–562
33. Biswas, T., Aihara, H., Radman-Livaja, M., Filman, D., Landy, A., and Ellenberger, T. (2005) A structural basis for allosteric control of DNA recombination by lambda integrase. *Nature* **435,** 1059–1066
34. Rice, P. A., Mouw, K. W., Montaño, S. P., Boocock, M. R., Rowland, S. J., and Stark, W. M. (2010) Orchestrating serine resolvases. *Biochem. Soc. Trans.* **38,** 384–387
35. Ninnemann, O., Koch, C., and Kahmann, R. (1992) The *E. coli fis* promoter is subject to stringent control and autoregulation. *EMBO J.* **11,** 1075–1083
36. Schneider, R., Travers, A., and Muskhelishvili, G. (2000) The expression of the *Escherichia coli fis* gene is strongly dependent on the superhelical density of DNA. *Mol. Microbiol.* **38,** 167–175
37. Blot, N., Mavathur, R., Geertz, M., Travers, A., and Muskhelishvili, G. (2006) Homeostatic regulation of supercoiling sensitivity coordinates transcription of the bacterial genome. *EMBO Rep.* **7,** 710–715
38. Ball, C. A., Osuna, R., Ferguson, K. C., and Johnson R. C. (1992) Dramatic changes in Fis levels upon nutrient upshift in *Escherichia coli*. *J. Bacteriol.* **174,** 8043–8056
39. Mallik, P., Pratt, T. S., Beach, M. B., Bradley, M. D., Undamatla, J., and Osuna, R. (2004) Growth phase-dependent regulation and stringent control of fis are conserved processes in enteric bacteria and involve a single promoter (fis P) in *Escherichia coli*. *J. Bacteriol.* **186,** 122–135
40. Nasser, W., Schneider, R., Travers, A., and Muskhelishvili, G. (2001) CRP modulates fis transcription by alternate formation of activating and repressing nucleoprotein complexes. *J. Biol. Chem.* **276,** 17878–17886
41. Crozat, E., Winkworth, C., Gaffé, J., Hallin, P. F., Riley, M. A., Lenski, R. E., and Schneider, D. (2010) Parallel genetic and phenotypic evolution of DNA superhelicity in experimental populations of *Escherichia coli*. *Mol. Biol. Evol.* **27,** 2113–2128
42. Nafissi, M., Chau, J., Xu, J., and Johnson, R. C. (2012) Robust translation of the nuceoid protein Fis requires a remote upstream AU element and is enhanced by RNA secondary structure. *J. Bacteriol.* **194,** 2458–2469
43. Jáuregui, R., Abreu-Goodger, C., Moreno-Hagelsieb, G., Collado-Vides, J., and Merino, E. (2003) Conservation of DNA curvature signals in regulatory regions of prokaryotic genes. *Nucleic Acids Res.* **31,** 6770–6777
44. Rivetti, C., Guthold, M., and Bustamante, C. (1999) Wrapping of DNA around the *E. coli* RNA polymerase open promoter complex. *EMBO J.* **18,** 4464–4475
45. Auner, H., Buckle, M., Deufel, A., Kutateladze, T., Lazarus, L., Mavathur, R., Muskhelishvili, G., Pemberton, I., Schneider, R., and Travers, A. (2003) Mechanism of transcriptional activation by FIS: role of core promoter structure and DNA topology. *J. Mol. Biol.* **331,** 331–344
46. Guérin, M., Leng, M., and Rahmouni, A. R. (1996) High resolution mapping of *E. coli* transcription elongation complex *in situ* reveals protein interactions with the non-transcribed strand. *EMBO J.* **15,** 5397–53407
47. Pratt, T. S., Steiner, T., Feldman, L. S., Walker, K. A., and Osuna, R. (1997) Deletion analysis of the fis promoter region in *Escherichia coli*: antagonistic effects of integration host factor and Fis. *J. Bacteriol.* **179,** 6367–6377
48. Meng, W., Belyaeva, T., Savery, N. J., Busby, S. J., Ross, W. E., Gaal, T., Gourse, R. L., and Thomas, M. S. (2001) UP element-dependent transcription at the *Escherichia coli* rrnB P1 promoter: positional requirements and role of the RNA polymerase $\alpha$ subunit linker. *Nucleic Acids Res.* **29,** 4166–4178
49. Rivetti, C., Guthold, M., and Bustamante, C. (1996) Scanning force microscopy of DNA deposited onto Mica: equilibration versus kinetic trapping studied by statistical polymer chain analysis. *J. Mol. Biol.* **264,** 919–932
50. Valle, F., Favre, M., De Los Rios, P., Rosa, A., and Dietler, G. (2005) Scaling exponents and probability distributions of DNA end-to-end distance. *Phys. Rev. Lett.* **95,** 158105
51. González-Gil, G., Bringmann, P., and Kahmann, R. (1996) FIS is a regulator of metabolism in *Escherichia coli*. *Mol. Microbiol.* **22,** 21–29
52. Kelly, A., Goldberg, M. D., Carroll, R. K., Danino, V., Hinton, J. C., and Dorman, C. J. (2004) A global role for Fis in the transcriptional control of metabolism and type III secretion in *Salmonella enterica* serovar *Typhimurium*. *Microbiology* **150,** 2037–2053
53. Maurer, S., Fritz, J., Muskhelishvili, G., and Travers, A. (2006) RNA polymerase and an activator form discrete subcomplexes in a transcription initiation complex. *EMBO J.* **25,** 3784–3790
54. Richardson, J. P. (1966) Some physical properties of RNA polymerase. *Proc. Natl. Acad. Sci. U.S.A.* **55,** 1616–1623
55. Chamberlin, M., McGrath, J., and Waskell, L. (1970) New RNA polymerase from *Escherichia coli* infected with bacteriophage T7. *Nature* **228,** 227–231
56. Savochkina, L. P., and Bibilashvili, R. Sh. (1979) Influence of ionic strength on RNA-polymerase structure. *Mol. Biol. (Mosk)* **13,** 509–518
57. Shaner, S. L., Piatt, D. M., Wensley, C. G., Yu, H., Burgess, R. R., and Record, M. T., Jr. (1982) Aggregation equilibria of *Escherichia coli* RNA polymerase: evidence for anion-linked conformational transitions in the protomers of core and holoenzyme. *Biochemistry* **21,** 5539–5551
58. Epshtein, V., and Nudler, E. (2003) Cooperation between RNA polymerase molecules in transcription elongation. *Science* **300,** 801–805
59. Epshtein, V., Toulmé, F., Rahmouni, A. R., Borukhov, S., and Nudler, E. (2003) Transcription through the roadblocks: the role of RNA polymerase cooperation. *EMBO J.* **22,** 4719–4727
60. Kansara, S. G., and Sukhodolets, M. V. (2011) Oligomerization of the *E. coli* core RNA polymerase: formation of ($\alpha 2\beta\beta'\omega$)2-DNA complexes and regulation of the oligomerization by auxiliary subunits. *PLoS One* **6,** e18990
61. Mechold, U., Potrykus, K., Murphy, H., Murakami, K. S., and Cashel, M. (2013) Differential regulation by ppGpp *versus* pppGpp in *Escherichia coli*.

*Nucleic Acids Res.* **41,** 6175–6189
62. Murakami K. S. (2013) X-ray crystal structure of *Escherichia coli* RNA polymerase σ70 holoenzyme. *J. Biol. Chem.* **288,** 9126–9134
63. Lang, B., Blot, N., Bouffartigues, E., Buckle, M., Geertz, M., Gualerzi, C. O., Mavathur, R., Muskhelishvili, G., Pon, C. L., Rimsky, S., Stella, S., Babu, M. M., and Travers, A. (2007) High affinity DNA binding sites for H-NS provide a molecular basis for selective silencing within proteobacterial genomes. *Nucleic Acids Res.* **35,** 6330–6337
64. Muskhelishvili, G., Travers, A. A., Heumann, H., and Kahmann, R. (1995) FIS and RNA polymerase holoenzyme form a specific nucleoprotein complex at a stable RNA promoter. *EMBO J.* **14,** 1446–1452
65. Ross, W., Gosink, K. K., Salomon, J., Igarashi, K., Zou, C., Ishihama, A., Severinov, K., and Gourse, R. L. (1993) A third recognition element in bacterial promoters: DNA binding by the α subunit of RNA polymerase. *Science* **262,** 1407–1413
66. Ross, W., Ernst, A., and Gourse, R. L. (2001) Fine structure of *E. coli* RNA polymerase-promoter interactions: α subunit binding to the UP element minor groove. *Genes Dev.* **15,** 491–506
67. Travers, A. A., Muskhelishvili, G., and Thompson, J. M. (2012) DNA information: from digital code to analogue structure. *Philos. Transact. A Math. Phys. Eng. Sci.* **370,** 2960–2986
68. Schneider, R., Travers, A., Kutateladze, T., and Muskhelishvili, G. (1999) A DNA architectural protein couples cellular physiology and DNA topology in *Escherichia coli*. *Mol. Microbiol.* **34,** 953–964
69. Ozoline, O. N., Deev, A. A., Arkhipova, M. V., Chasov, V. V., and Travers, A. (1999) Proximal transcribed regions of bacterial promoters have a non-random distribution of A/T tracts. *Nucleic Acids Res.* **27,** 4768–4774
70. Menendez, M., Kolb, A., and Buc, H. (1987) A new target for CRP action at the malT promoter. *EMBO J.* **6,** 4227–4234
71. Zhang, X., and Bremer, H. (1996) Effects of Fis on ribosome synthesis and activity and on rRNA promoter activities in *Escherichia coli*. *J. Mol. Biol.* **259,** 27–40
72. Nilsson, L., Verbeek, H., Vijgenboom, E., van Drunen, C., Vanet, A., and Bosch, L. (1992) FIS-dependent trans activation of stable RNA operons of *Escherichia coli* under various growth conditions. *J. Bacteriol.* **174,** 921–929
73. Nilsson, L., Verbeek, H., Hoffmann U., Haupt, M., and Bosch, L. (1992) Inactivation of the *fis* gene leads to reduced growth rate. *FEMS Microbiol. Lett.* **78,** 85–88
74. Bordes, P., Conter, A., Morales, V., Bouvier, J., Kolb, A., and Gutierrez, C. (2003) DNA supercoiling contributes to disconnect σS accumulation from σS-dependent transcription in *Escherichia coli*. *Mol. Microbiol.* **48,** 561–571
75. Muskhelishvili, G., Sobetzko, P., Geertz, M., and Berger, M. (2010) General organizational principles of the transcriptional regulation system: a tree or a circle? *Mol. Biosyst.* **6,** 662–676
76. Geertz, M., Travers, A., Mehandziska, S., Sobetzko, P., Chandra-Janga, S., Shimamoto, N., and Muskhelishvili, G. (2011) Structural coupling between RNA polymerase composition and DNA supercoiling in coordinating transcription: a global role for the ω subunit? *MBio* **2,** e00034–11
77. Muskhelishvili, G., and Travers, A. (2010) FIS and nucleoid dynamics upon exit from lag phase. in *Bacterial Chromatin* (Dame, R., and Dorman, C., eds) pp. 323–352, Springer, New York
78. Walker, K. A., Mallik, P., Pratt, T. S., and Osuna, R. (2004) The *Escherichia coli* Fis promoter is regulated by changes in the levels of its transcription initiation nucleotide CTP. *J. Biol. Chem.* **279,** 50818–50828
79. Kolmsee, T., Delic, D., Agyenim, T., Calles, C., and Wagner, R. (2011) Differential stringent control of *Escherichia coli* rRNA promoters: effects of ppGpp, DksA and the initiating nucleotides. *Microbiology* **157,** 2871–2879
80. Marinello, J., Chillemi, G., Bueno, S., Manzo, S. G., and Capranico, G. (2013) Antisense transcripts enhanced by camptothecin at divergent CpG-island promoters associated with bursts of topoisomerase I-DNA cleavage complex and R-loop formation. *Nucleic Acids Res.* **41,** 10110–10123
81. Naughton, C., Corless, S., and Gilbert, N. (2013) Divergent RNA transcription: a role in promoter unwinding? *Transcription* **4,** 162–166
82. Hu, H. Y., He, L., and Khaitovich, P. (2014) Deep sequencing reveals a novel class of bidirectional promoters associated with neuronal genes. *BMC Genomics* **15,** 457
83. Necas, D., and Klapetek, P. (2012) Gwyddion: an open-source software for SPM data analysis. *Cent. Eur. J. Phys.* **10,** 181–188
84. Tichopad, A., Dzidic, A., and Pfaffl, M. W. (2002) Improving quantitative real-time RT-PCR reproducibility by boosting primer-linked amplification efficiency. *Biotechnol. Lett.* **24,** 2053–2056